

# DSCR1 is required for both axonal growth cone extension and steering

Wei Wang,<sup>1\*</sup> Asit Rai,<sup>1\*</sup> Eun-Mi Hur,<sup>2,3,4</sup> Zeev Smilansky,<sup>5</sup> Karen T. Chang,<sup>6,7</sup> and Kyung-Tai Min<sup>1</sup>

<sup>1</sup>Department of Biological Sciences, School of Life Sciences, Ulsan National Institute of Science and Technology, Ulsan 44919, Korea

<sup>2</sup>Brain Science Institute-Center for Neuroscience and <sup>3</sup>Convergence Research Center for Diagnosis, Treatment and Care System of Dementia, Korea Institute of Science and Technology, Seoul 02792, Korea

<sup>4</sup>Department of Neuroscience, University of Science and Technology, Daejeon 34113, Korea

<sup>5</sup>Animax Biotech, Ltd., Tel-Aviv 69710, Israel

<sup>6</sup>Zilkha Neurogenetic Institute and <sup>7</sup>Department of Cell and Neurobiology, University of Southern California, Los Angeles, CA 90089

Local information processing in the growth cone is essential for correct wiring of the nervous system. As an axon navigates through the developing nervous system, the growth cone responds to extrinsic guidance cues by coordinating axon outgrowth with growth cone steering. It has become increasingly clear that axon extension requires proper actin polymerization dynamics, whereas growth cone steering involves local protein synthesis. However, molecular components integrating these two processes have not been identified. Here, we show that Down syndrome critical region 1 protein (DSCR1) controls axon outgrowth by modulating growth cone actin dynamics through regulation of cofilin activity (phospho/dephospho-cofilin). Additionally, DSCR1 mediates brain-derived neurotrophic factor-induced local protein synthesis and growth cone turning. Our study identifies DSCR1 as a key protein that couples axon growth and pathfinding by dually regulating actin dynamics and local protein synthesis.

## Introduction

The ability of an axon to navigate through the developing nervous system depends on the growth cone. In response to extrinsic cues, a growth cone exhibits changes in elongation rate and direction en route to its final destination (Buck and Zheng, 2002; Dent et al., 2011; Jung et al., 2012; Vitriol and Zheng, 2012). Extrinsic cues control growth cone motility through an array of signaling cascades that control actin and microtubule dynamics to regulate growth cone advance and steering (Dent et al., 1999; Schaefer et al., 2002, 2008; Kornack and Giger, 2005; Lowery and Van Vactor, 2009; Vitriol and Zheng, 2012). The regulation of actin polymerization/depolymerization is vital for axon growth and guidance. However, the molecular components mediating this process have not been completely defined. One key protein is cofilin, which regulates axon growth by severing and depolymerizing actin filaments. Increasing cofilin activity has been shown to promote neurite extension (Dent et al., 2011), but on the contrary, higher cofilin activity has been associated with growth cone collapse (Aizawa et al., 2001; Hsieh et al., 2006; Piper et al., 2006). Additionally, knockdown of LIM kinases that inactivate cofilin by phosphorylation resulted in inhibition of neurite outgrowth in chick dorsal root ganglion neurons (Endo et al., 2007). These studies thus suggest that cofilin has dual effects on growth cone motility. To reconcile the

apparent controversy, it has been proposed that the unique cytosolic environment of a particular growth cone, such as basal actin dynamics and the ratio of cofilin to actin monomer, might determine the effect of cofilin (in)activation on growth cone behavior (Vitriol and Zheng, 2012).

It has also been shown that local synthesis of  $\beta$ -actin in the developing growth cone in response to external stimuli is important for axon guidance and migration (Leung et al., 2006; Yao et al., 2006), and several regulators that mediate local mRNA translation at axonal growth cones, such as the zipcode binding protein 1 (ZBP1), have been identified (Leung et al., 2006; Yao et al., 2006; Willis et al., 2007; Welshhans and Basell, 2011). Also, brain-derived neurotrophic factor (BDNF) has been shown to induce local  $\beta$ -actin translation during axon development, but the molecular mechanisms involved in local protein synthesis remain to be defined. Despite the identification of numerous proteins that control axonal growth cone development, our knowledge of the components that mediate actin dynamics and axon guidance is not complete.

The Down syndrome critical region 1 protein (DSCR1, also called regulator of calcineurin [RCAN1]) is located on chromosome 21 and is highly expressed in hippocampal neurons (Fuentes et al., 1995). DSCR1 belongs to a conserved family of calcineurin inhibitors called calcipressins, which

\*W. Wang and A. Rai contributed equally to this paper.

Correspondence to Kyung-Tai Min: ktainmin@unist.ac.kr

Abbreviations used in this paper: BDNF, brain-derived neurotrophic factor; CsA, cyclosporin A; DIV, day in vitro; DSCR1, Down syndrome critical region 1 protein; FMRP, Fragile X mental retardation protein; FRET, Förster resonance energy transfer; G-actin, globular actin; ZBP1, zipcode binding protein 1.

© 2016 Wang et al. This article is distributed under the terms of an Attribution-Noncommercial-Share Alike-No Mirror Sites license for the first six months after the publication date (see <http://www.rupress.org/terms>). After six months it is available under a Creative Commons License (Attribution-Noncommercial-Share Alike 3.0 Unported license, as described at <http://creativecommons.org/licenses/by-nc-sa/3.0/>).

includes RCN1P in yeast (Kingsbury and Cunningham, 2000), CBP1 in fungus (Görlach et al., 2000), nebula in *Drosophila melanogaster* (Chang et al., 2003), and DSCR1 in mouse and human (Casas et al., 2001; Arron et al., 2006). DSCR1 also interacts with Fragile X mental retardation protein (FMRP), an RNA-binding protein that controls mRNA transport and translation, including local translation in dendritic spines (Wang et al., 2012). Absence of FMRP is responsible for Fragile X syndrome (Santoro et al., 2012). It has been suggested that Down syndrome and Fragile X syndrome participate in common biological pathways leading to intellectual disability (Chang et al., 2013). Here we demonstrate a previously unidentified role for DSCR1 in regulating axonal growth cone extension and growth cone turning toward an attractant signal. Our work reveals that DSCR1 regulates the ratio of cofilin and phospho-cofilin to modulate axon outgrowth as well as mediates BDNF-induced local protein synthesis to regulate growth cone turning.

## Results

### DSCR1 plays an important role in axon development and axonal growth cone steering

In initial studies we demonstrated that DSCR1 is highly expressed in the growth cones of mouse primary hippocampal neurons (Fig. S1, A–E). This suggests that DSCR1 may help regulate axon growth and/or guidance. Immunostaining revealed that wild-type hippocampal neurons at day in vitro (DIV) 3 were clearly polarized with distinguishable dendrites and an axon, which were marked by antibodies against MAP2 and Tau1, respectively (Fig. 1 A). At this time, *DSCR1*<sup>−/−</sup> neurons had also extended an identifiable but shorter axon. In contrast, neurons from a *DSCR1* transgenic line that overexpresses DSCR1 extended axons that were longer than those from wild-type neurons (Fig. 1, A and B). To more accurately assess the role of DSCR1 in axon development, we monitored axon growth by time-lapse imaging for 12 h starting at DIV 2 (Fig. S1, F and G). Results show that absence of DSCR1 reduces and overexpression of DSCR1 increases the rate of axon growth compared with the rate observed in wild-type control neurons. In addition, the morphologies of *DSCR1*<sup>−/−</sup> axons were abnormal, exhibiting ruffling and extensive process elaboration.

To determine if DSCR1 also affects growth cone steering, we examined the behaviors of axons of wild-type, *DSCR1*<sup>−/−</sup>, and *DSCR1* transgenic mice in Dunn chambers in the presence or absence of a gradient of BDNF (Yam et al., 2009; Fig. 1, C and D). Over a 2-h period, we measured the turning angles of individual axonal growth cones (Fig. 1, C–E). The growth cones from control and *DSCR1* transgenic mice turned toward the BDNF gradient. *DSCR1*<sup>−/−</sup> axons, however, exhibited less growth cone extension and failed to turn toward the source of BDNF (Fig. 1, C–E). Increased levels of DSCR1 also shortened the time required to observe initial turning of a growth cone (Fig. 1 F); turning was observed in growth cones from *DSCR1* transgenic mice in ~10 min, whereas ~20 min were required to observe turning by wild-type growth cones. In contrast, growth cones from *DSCR1*<sup>−/−</sup> mice did not respond to the BDNF gradient during the entire 2-h long recording period. Together, these results indicate that DSCR1 is required for both axon growth and growth cone steering.

### DSCR1 regulates axonal growth cone dynamics by modulating the levels of phospho-cofilin and cofilin

To further examine growth cone extension and steering in axons lacking or overexpressing *DSCR1*, we performed short-term live imaging of axonal growth cones at DIV 3 and investigated dynamics of filopodia-containing lifeact-GFP (F-actin) and RFP-actin (globular actin [G-actin], F-actin, or total actin; Fig. 2 A). Formation of actin filaments (F-actin) depends on the availability of monomeric G-actin. Ratios of filamentous to G-actin were quantified using fluorescent conjugates of cytochalasin and vitamin D-binding protein, respectively (Van Baelen et al., 1980; Fishkind and Wang, 1993; Lee et al., 2013). Interestingly, compared with those of wild-type neurons, filopodia in growth cones overexpressing *DSCR1* had a high F-actin/G-actin ratio and high motility, whereas filopodia of *DSCR1*-deficient neurons had a low F-actin/G-actin ratio and low motility. Consequently, we hypothesized that DSCR1-dependent modulation of growth cone dynamics results from the alterations of the ratio of F- and G-actin, resulting in fast or slow axon growth. Data presented in Fig. 2 C show that the F-actin level in the leading edge of filopodia of neurons overexpressing *DSCR1* was dramatically higher than levels in wild-type and *DSCR1*<sup>−/−</sup> growth cones.

Because the activity of the F-actin–severing protein cofilin, which can be assessed by measurement of the cofilin/phospho-cofilin ratio, is crucial for maintaining the balance between F-actin and G-actin, we next compared the levels of cofilin and phospho-cofilin in wild-type, *DSCR1*-deficient, and *DSCR1*-overexpressing growth cones to determine whether differences in active (dephospho)-cofilin correlate with the differences in F-actin and G-actin observed above. Indeed, *DSCR1*<sup>−/−</sup> growth cones showed significantly higher cofilin/phospho-cofilin ratios than those of wild-type growth cones, and *DSCR1*-overexpressing growth cones exhibited a lower cofilin/phospho-cofilin ratio, reflecting reduced cofilin activity (Fig. 2, D and E). These findings are consistent with the notion that increased levels of active (dephospho)-cofilin in *DSCR1*<sup>−/−</sup> axonal growth cone decrease the F-actin/G-actin ratio, resulting in impaired axonal growth cone extension.

Next, to investigate if cofilin activity indeed regulates axon growth, we attempted to suppress the impact of DSCR1 deficiency on the cofilin/phospho-cofilin ratio in *DSCR1*<sup>−/−</sup> growth cones. It is known that DSCR1 inhibits the protein phosphatase calcineurin, which dephosphorylates phospho-cofilin, thereby activating it (Fuentes et al., 2000; Zhou et al., 2004; Wang et al., 2005). In past work, we have shown that DSCR1 regulates dendritic spine morphogenesis by inactivating calcineurin and the level of phospho-cofilin (Wang et al., 2012). Therefore, we first examined if suppression of calcineurin activity by cyclosporin A (CsA) treatment restores the relative levels of cofilin to phospho-cofilin and F-actin/G-actin ratios as well as the length of the *DSCR1*<sup>−/−</sup> axons. As expected, we found that treatment of *DSCR1*<sup>−/−</sup> neurons with CsA increased the level of phospho-cofilin, but surprisingly reduced the total level of cofilin. Additionally, CsA treatment also restored the F-actin/G-actin ratio to a ratio similar to that in wild-type growth cones (Fig. 3). To further confirm the impact of DSCR1-mediated calcineurin inhibition on axon growth, *DSCR1*<sup>−/−</sup> neurons were treated with CsA from DIV 1 until DIV 3 and stained for axonal and dendritic markers. Treatment of *DSCR1*<sup>−/−</sup> neurons with CsA clearly promoted axon outgrowth (Fig. 4, A and B), suggesting that DSCR1 mediates axon growth through regulation of calcineurin. To

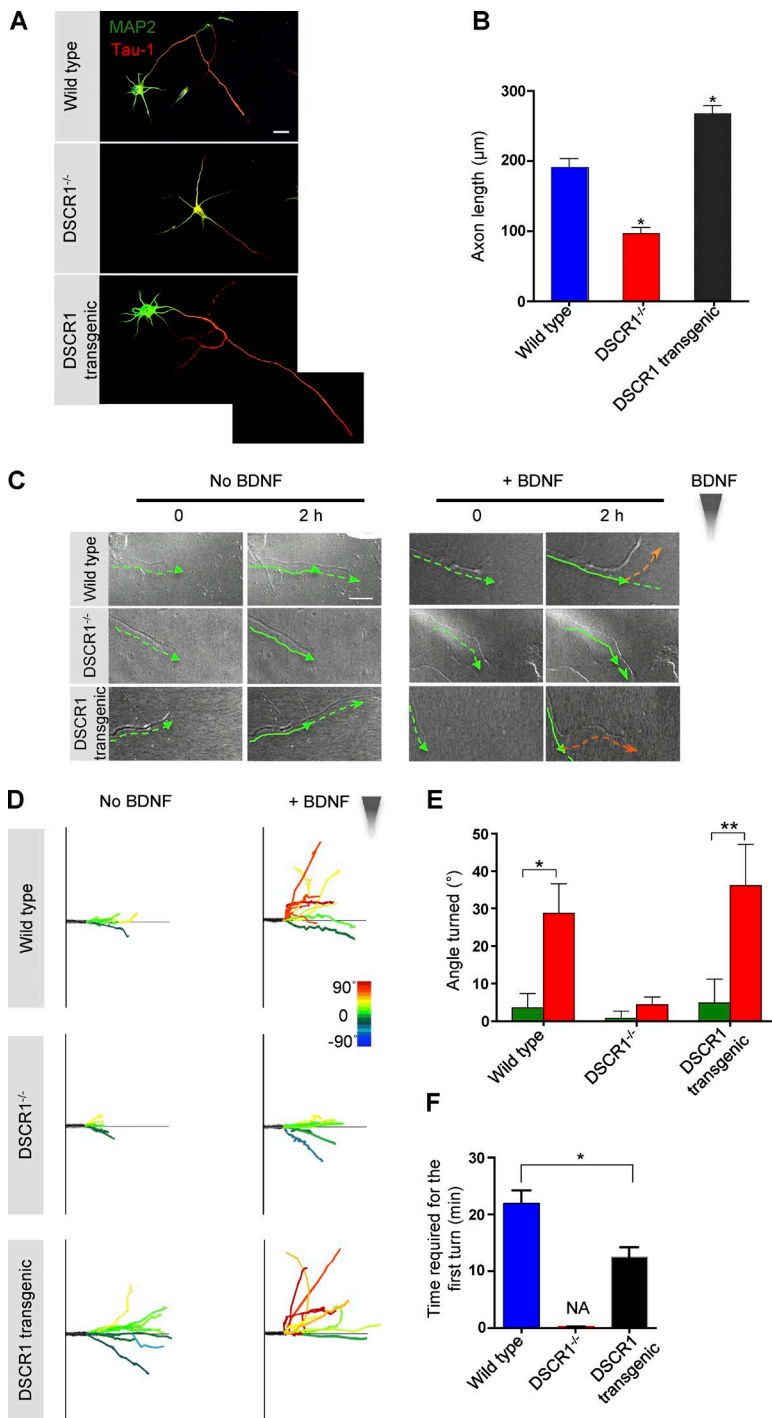


**Figure 1. DSCR1 is necessary for axon development.** (A and B) DSCR1 regulates axon outgrowth. Hippocampal primary neurons from wild-type, *DSCR1*<sup>-/-</sup>, and *DSCR1* transgenic mice were cultured *in vitro* for 3 d (DIV 3) and immunostained with MAP2 and Tau-1 antibodies to identify dendrites and axons, respectively. *DSCR1*<sup>-/-</sup> neurons also extended an identifiable but shorter axon by DIV 3, whereas *DSCR1* transgenic neurons extended longer axons compared with those of wild type.  $n = 22$  for each condition. \*,  $P < 0.0001$ . Bar, 20  $\mu$ m. (C) Growth cone steering in a Dunn chamber with or without BDNF. Lines drawn below the axons show the paths of growth cones. Bar, 10  $\mu$ m. (D) Trajectory plots showed growth cone turning responses of individual neurons of wild-type, *DSCR1*<sup>-/-</sup>, and *DSCR1* transgenic mice. BDNF gradient is established to increase along the y axis, and all axons are repositioned to it accordingly for clarity. Black lines show the initial 10  $\mu$ m of axons, and different colors represent the initial turning angles of the axon growth cones over a 2-h recording period. To reduce complexity of the figure, only 10 representative traces are shown.  $n = 23$  for wild type,  $n = 10$  for *DSCR1*<sup>-/-</sup>, and  $n = 14$  for *DSCR1* transgenic neurons were analyzed. (E) Axonal growth cones of wild-type and *DSCR1* transgenic neurons showed increased turning responses in the presence of BDNF, whereas *DSCR1*<sup>-/-</sup> axon growth cones showed little turning. \*,  $P < 0.02$ ; \*\*,  $P < 0.05$ . (F) *DSCR1* transgenic axon growth cones turned faster toward BDNF compared with wild type, whereas *DSCR1*<sup>-/-</sup> show little turning. \*,  $P < 0.002$ . Values shown are mean  $\pm$  SEM and are tested for statistical significance by *t* test.

further verify that DSCR1 plays a key role in axon outgrowth, we compared the effects of CsA on wild-type and *DSCR1*-overexpressing neurons. We found that treatment of wild-type neurons with CsA reduced the ratio of cofilin/phospho-cofilin and increased both the F-actin/G-actin ratio and mean axonal length (Fig. S2, A, B, and E–G). In contrast, CsA treatment of *DSCR1* transgenic neurons did not increase the ratio of cofilin/phospho-cofilin, reduce the F-actin/G-actin ratio, or further reduce the mean length of axons (Fig. S2, C, D, and H–J). Our observation that CsA has little effect on the growth cones and axons of *DSCR1*-overexpressing neurons argues that calcineurin inhibition by DSCR1 plays a key role in regulating axon growth.

#### DSCR1-mediated regulation of the growth cone turning response to BDNF is independent of the level of cofilin/phospho-cofilin

To determine whether calcineurin inhibition by DSCR1 also mediates the chemoattractant response of growth cones to BDNF, we examined the turning responses of growth cones in a Dunn chamber in the presence of a BDNF gradient. CsA treatment of *DSCR1*<sup>-/-</sup> neurons significantly increased axon outgrowth, but did not alter the insensitivity of the growth cones of these neurons to a BDNF gradient (Fig. 4, C and D), suggesting that regulation of calcineurin by DSCR1 does not affect

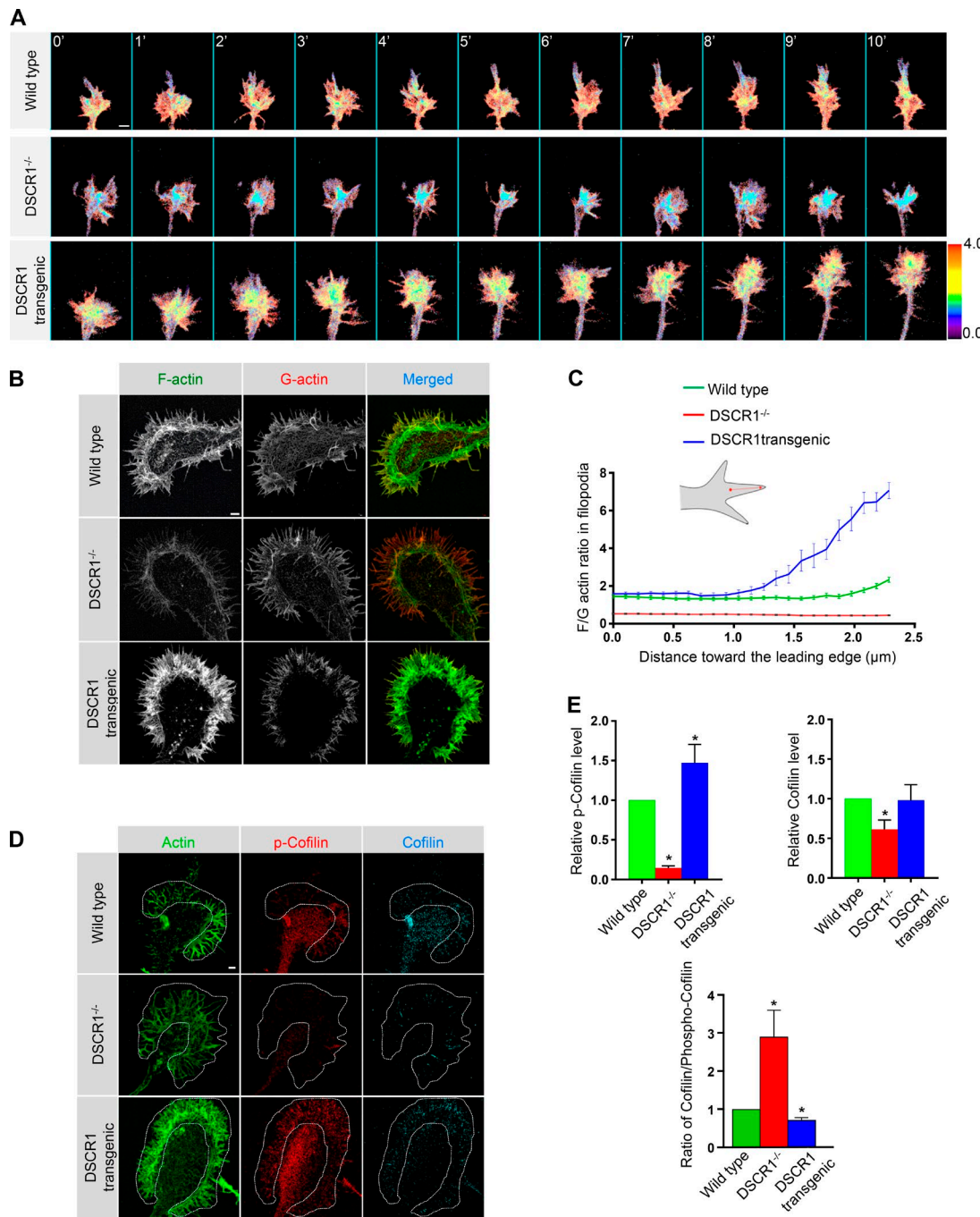


**Figure 2. DSCR1 mediates the axonal growth cone dynamics.** (A) Pseudo-colored images of axonal growth cone dynamics for wild-type, *DSCR1*<sup>-/-</sup>, and *DSCR1* transgenic neurons containing lifeact-GFP and RFP-actin shown at every 1-min interval. Higher values in the color scale indicate more F-actin presence than G-actin in the growth cone. Axonal growth cone dynamics were monitored using dual-channel time-lapse imaging of total actin (G-actin and F-actin, RFP-actin) and filamentous actin (lifeact-GFP). Images were taken at 5-s intervals for 10 min. (B and C) Axonal growth cones of wild type, *DSCR1*<sup>-/-</sup>, and *DSCR1* transgenic were labeled for actin filaments (F-actin) and monomeric G-actin by using fluorescent phalloidin and antibodies against vitamin D-binding protein. Bar, 2  $\mu$ m. The ratio of F-actin/G-actin in filopodia of wild-type, *DSCR1*<sup>-/-</sup>, and *DSCR1* transgenic axonal growth cones was analyzed.  $n = 28$  (42) for wild-type growth cone,  $n = 24$  (45) for *DSCR1*<sup>-/-</sup>, and  $n = 24$  (48) for *DSCR1* transgenic. Parentheses indicate the number of filopodia. (D and E) Axonal growth cones of wild type, *DSCR1*<sup>-/-</sup>, and *DSCR1* transgenic were stained with antibodies against cofilin and phospho-cofilin. Bar, 2  $\mu$ m. The level of phospho-cofilin in the peripheral region of axonal growth cone is significantly decreased in *DSCR1*<sup>-/-</sup> compared with that of wild type and *DSCR1* transgenic.  $n = 22$  for each condition. \*,  $P < 0.001$ . Values shown are mean  $\pm$  SEM and are tested for statistical significance by *t* test.

growth cone chemoattractant responsiveness. This result is also consistent with the effect of calcineurin on the cofilin/phospho-cofilin ratio (Fig. 3). Note that wild-type and *DSCR1*<sup>-/-</sup> neurons also did not alter phospho-cofilin or cofilin levels after BDNF treatment (Fig. S4, A–D).

To further verify the absence of an impact of the cofilin/phospho-cofilin ratio on the chemoattractant response of growth cones to BDNF, we examined axonal length and growth cone turning in neurons in which the phosphomimetic mutant of cofilin (*cofilin S3E*) was overexpressed. Overexpression of *cofilin*

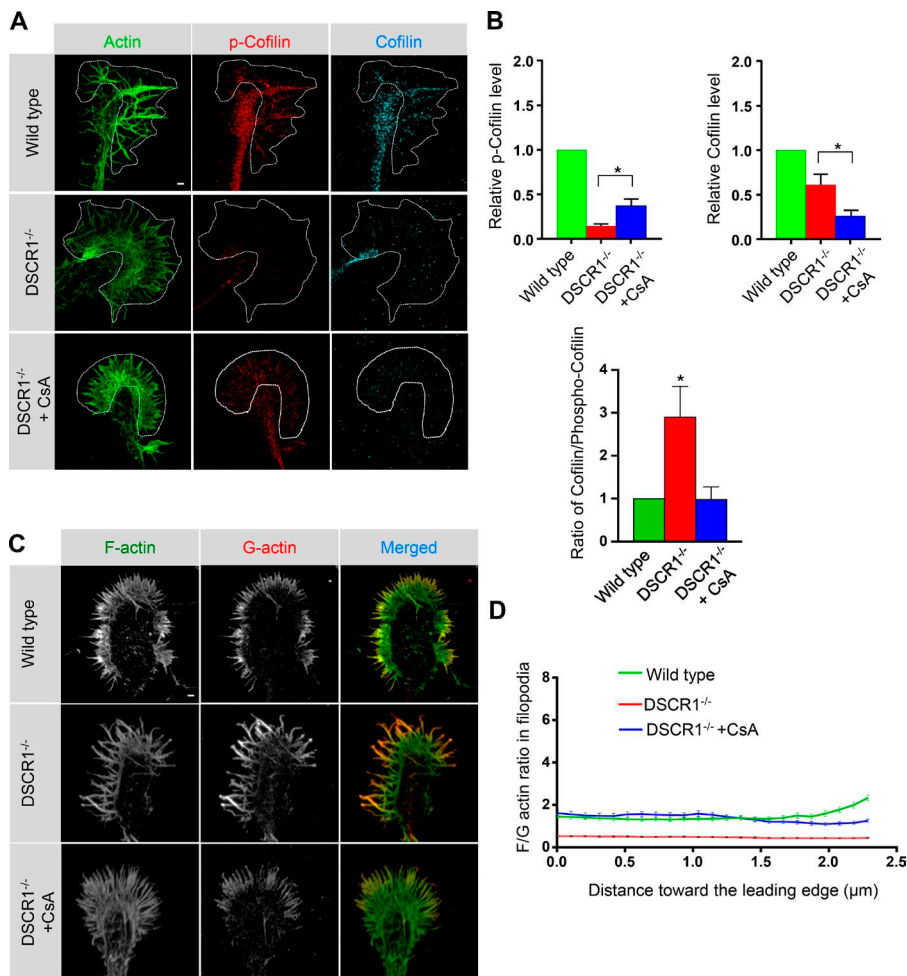


**Figure 3. DSCR1 mediates axonal outgrowth by modulating the level of cofilin phosphorylation.** (A and B) Axonal growth cones of wild type, *DSCR1*<sup>-/-</sup>, and *DSCR1*<sup>-/-</sup> treated with CsA were stained with antibodies against cofilin and phospho-cofilin. Bar, 2 μm. Treatment of *DSCR1*<sup>-/-</sup> neurons with CsA increased the level of phospho-cofilin and restored the ratio of cofilin and phospho-cofilin.  $n = 22$  for each condition. \*,  $P < 0.001$ . (C) F-actin and G-actin were shown by using fluorescent phalloidin and antibodies against vitamin D-binding protein. Bar, 2 μm. (D) The ratio of F-actin/G-actin in filopodia of wild-type, *DSCR1*<sup>-/-</sup>, and *DSCR1*<sup>-/-</sup> neurons treated with CsA was analyzed.  $n = 28$  (42) for wild-type growth cone,  $n = 24$  (45) for *DSCR1*<sup>-/-</sup>, and  $n = 16$  (45) for *DSCR1*<sup>-/-</sup> with CsA. Parentheses indicate the number of filopodia. Values shown are mean ± SEM and are tested for statistical significance by *t* test.

*S3E* reduces dephosphorylation of endogenous phospho-cofilin through competition with phosphatases, thereby elevating the ratio of phospho-cofilin to cofilin. As expected, *cofilin S3E* overexpression in *DSCR1*-deficient neurons resulted in significantly greater axon growth. In contrast, *cofilin S3E* overexpression did not restore the ability of these growth cones to respond to a chemoattractive gradient of BDNF (Fig. 4, E–G). Consistent with this, overexpression of *cofilin S3E* in wild-type neurons increased axonal growth but did not appear to further enhance the responsiveness of growth cones to a BDNF gradient (Fig. S3, E–G). Together, these results suggest that DSCR1 can regulate axon outgrowth, but not chemotropic factor responsiveness by influencing the relative levels of phospho-cofilin and cofilin.

#### DSCR1 is required for local protein synthesis in axonal growth cone

Recent data have established an important role for local protein synthesis in the growth cone in the responsiveness of growth cones to chemotropic factors (Brittis et al., 2002; Tcherkezian et al., 2010; Jung et al., 2012). Previously, we showed that the DSCR1 protein is enriched in dendritic spines, and through interaction with the mRNA binding protein FMRP modulates local protein synthesis in dendritic spines, thereby regulating spine morphology (Wang et al., 2012). Consequently, we hypothesized that, similar to its role in spine morphogenesis, DSCR1 may control the responsiveness of growth cones to chemoattractants, such as BDNF, through regulation of local protein synthesis. We

first determined whether DSCR1 regulates local protein synthesis in growth cones by applying a recently reported technique termed proteins synthesis monitoring. This technique allows for quantitative analysis of protein synthesis and detection of active ribosomes through assessment of occupancy of adjacent sites on ribosomes by tRNAs labeled with Förster resonance energy transfer (FRET) acceptor and donor fluorophores (Barhoom et al., 2011). We transfected primary hippocampal neurons prepared from wild-type, *DSCR1*<sup>-/-</sup>, or *DSCR1* transgenic mice with bulk uncharged tRNA labeled with either Cy3 or rhodamine 110 (Rho110). To assess local protein synthesis, we measured FRET signals between Cy3-tRNA (acceptor) and Rho110-tRNA (donor) after acceptor photobleaching. FRET signals arise when two fluorescent tRNAs occupy adjacent sites on the ribosome, so an increase in the FRET signal reflects active protein synthesis originating from the proximity of FRET pairs on translational machinery (Barhoom et al., 2011). We found that BDNF treatment induced a significant increase in FRET signal in axonal growth cones of DIV 3 neurons from wild-type mice (Fig. 5, A and B). The addition of puromycin, a translational inhibitor, extinguished the BDNF-induced FRET signals (Fig. S4, A and B), indicating that BDNF-induced changes in FRET signals result from local protein synthesis at axonal growth cones. Next, we monitored BDNF-induced local protein synthesis at axonal growth cones of *DSCR1*-deficient and -overexpressing neurons. No detectable FRET signal was observed after BDNF application in growth cones lacking *DSCR1*, whereas application of BDNF

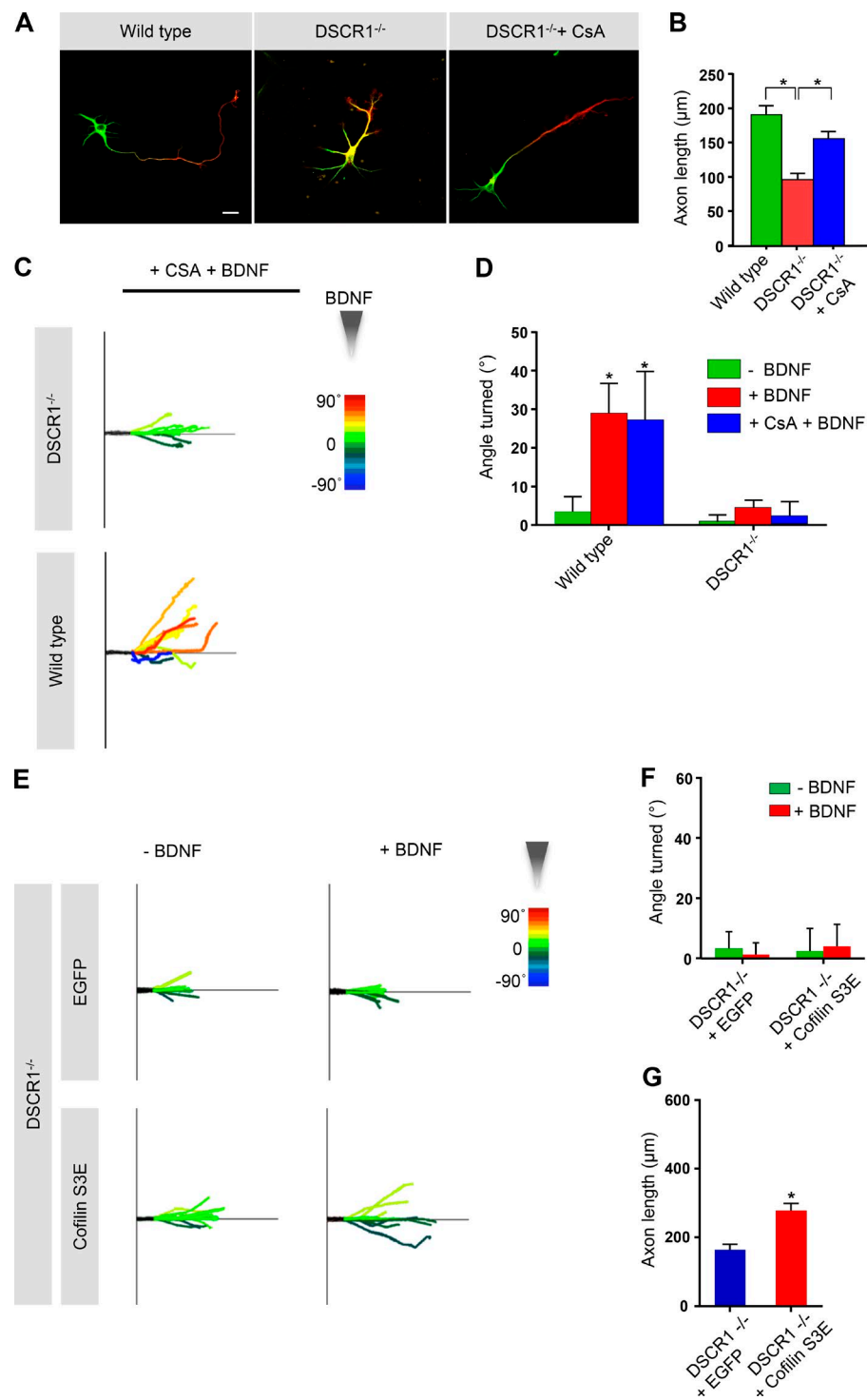


**Figure 4. DSCR1-mediated axonal growth cone steering is independent of growth cone extension, and cofilin S3E overexpression in DSCR1<sup>-/-</sup> neurons extends axon length but not axonal growth turning toward BDNF.** (A and B) Hippocampal primary neurons of wild-type, DSCR1<sup>-/-</sup>, and DSCR1<sup>-/-</sup> neurons treated with CsA were cultured in vitro for 3 d (DIV 3) and immunostained with MAP2 and Tau-1 antibodies to identify dendrites and axons, respectively. DSCR1<sup>-/-</sup> neurons extended an identifiable but shorter axon, whereas DSCR1<sup>-/-</sup> neurons treated with CsA has clearly developed and extended axons.  $n = 22$  for each condition. \*,  $P < 0.001$ . Bar, 20  $\mu$ m. (C and D) Growth cone steering in a Dunn chamber with or without BDNF. Trajectory plots showed growth cone turning responses of individual neurons of DSCR1<sup>-/-</sup> treated with CsA at DIV 3. Results from the Dunn chamber assay clearly showed that CsA did not rescue the defective axonal growth cone turning phenotype in DSCR1<sup>-/-</sup> neurons.  $n > 18$  for each condition. \*,  $P < 0.05$ . Values shown are mean  $\pm$  SEM and are tested for statistical significance by *t* test. (E) DSCR1<sup>-/-</sup> axonal growth cones were transfected with cofilin S3E overexpression plasmid and then placed in Dunn chamber with or without BDNF. Trajectory plots show growth cone turning response of individual neurons of DSCR1<sup>-/-</sup> overexpressing cofilin S3E. (F) Overexpression of cofilin S3E showed no effect on axonal growth turning response to BDNF.  $n > 10$  for each condition. (G) Axon length was significantly increased in DSCR1<sup>-/-</sup> neurons overexpressing cofilin S3E.  $n = 35$  for DSCR1<sup>-/-</sup> overexpressing EGFP and  $n = 30$  for DSCR1<sup>-/-</sup> overexpressing cofilin S3E. \*,  $P < 0.0001$ . Values shown are mean  $\pm$  SEM and are tested for statistical significance by *t* test.

to the growth cones from *DSCR1* transgenic mice dramatically increased the FRET signal (Fig. 5, A and B). These data imply that DSCR1 is required for BDNF-dependent local protein synthesis in growth cones. Because local synthesis of  $\beta$ -actin in growth cones has been shown to be essential for chemotactic responses of growth cones to both netrin and BDNF (Leung et al., 2006; Yao et al., 2006), we next examined whether local  $\beta$ -actin mRNA translation is controlled by DSCR1. To this end, we constructed a vector containing the photoswitchable dendra-2 protein fused with the 3'UTR of  $\beta$ -actin mRNA together with two copies of the palmitoylation sequence (*dendra2-3*

UTR of  $\beta$ -actin), similar to previous studies (Welshans and Bassell, 2011; Wang et al., 2012). The 3'UTR of the  $\beta$ -actin transcript was sufficient to guide its localization to the axonal growth cone, and newly synthesized dendra-2 protein was monitored after photoconversion and BDNF application. UV light was illuminated on axonal growth cones, which irreversibly converted the green fluorescent dendra-2 to RFP. Newly synthesized green fluorescent dendra-2 proteins in axonal growth cones were quantified from time-lapse images taken every 10 min for 60 min after BDNF application (Fig. 5, C–E). Upon BDNF stimulation, newly synthesized green fluorescent dendra-2 was detected in

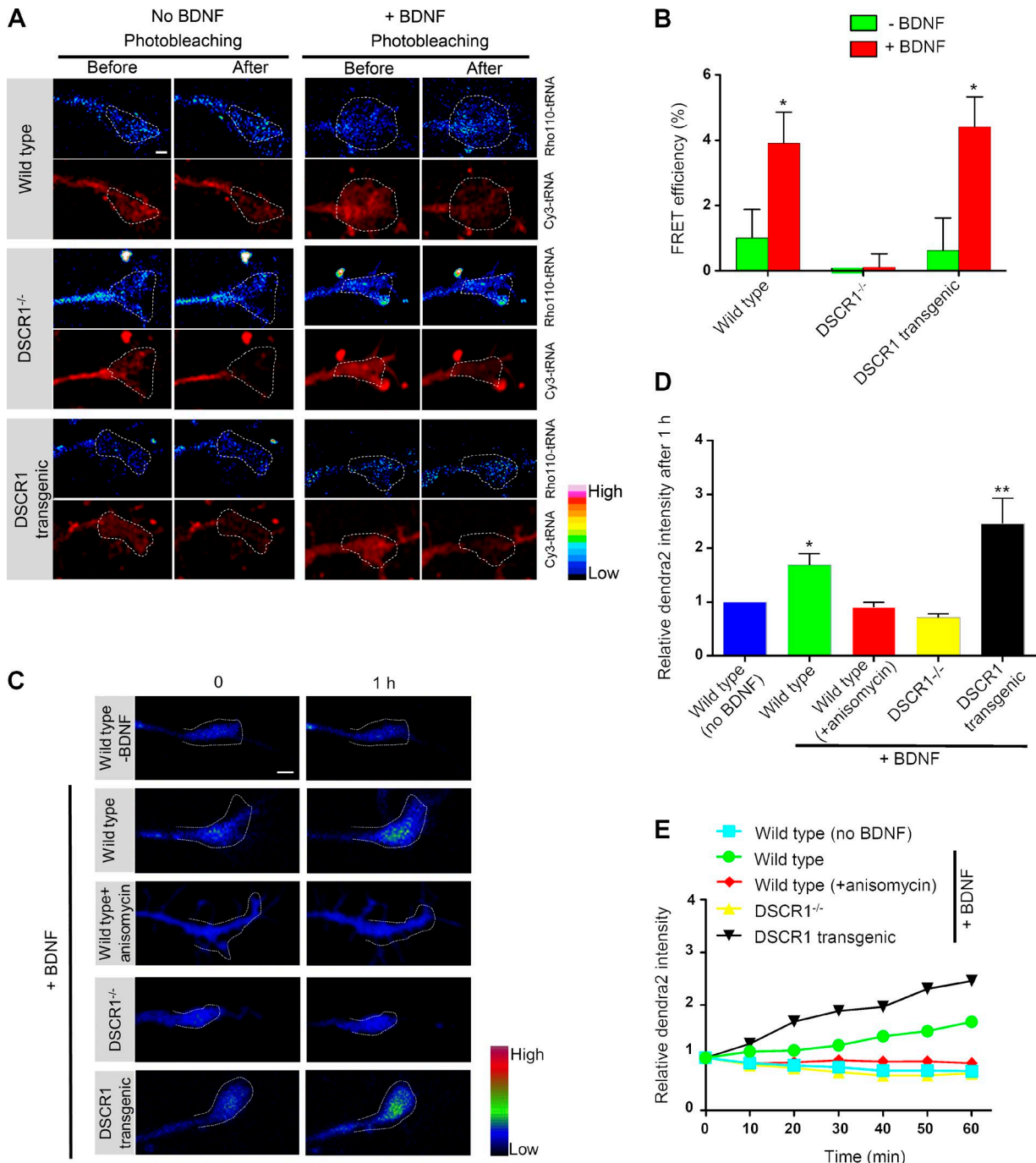


**Figure 5. DSCR1 is required for local protein synthesis in axonal growth cones.** (A and B) Hippocampal primary neurons of wild-type, *DSCR1<sup>-/-</sup>*, and *DSCR1* transgenic mice were transfected with bulk Cy3-labeled tRNAs and Rho-110-labeled tRNAs. FRET signals are generated when a donor-labeled tRNA is positioned next to an acceptor-labeled tRNA in an active ribosome. Cy3-tRNAs (acceptor) and Rho-110-tRNA (donor) signals were measured both before and after photobleaching to estimate FRET signal intensity. Significantly higher FRET signals were detected in the axonal growth cones when neurons of wild-type and *DSCR1* transgenic mice were treated with BDNF, whereas no FRET signal was detected in *DSCR1<sup>-/-</sup>* axonal growth cones. Dotted line indicates axonal growth cone and the photobleached area. Pseudo-colored images show the relative fluorescence intensity. Experiments were performed at DIV 3.  $n > 20$  axonal growth cones were analyzed for each condition. \*,  $P < 0.05$ . Values are shown as mean  $\pm$  SEM and are tested for statistical significance by *t* test. Bar, 2  $\mu$ m. (C) Pseudo-colored images of the dendra2-3 UTR of  $\beta$ -actin vector. Increased intensity of dendra-2 represents local protein synthesis in axonal growth cones. (D and E) Consistent with the results in A, axonal growth cones of *DSCR1* transgenic and wild type treated with BDNF showed high fluorescent intensity, suggesting an increase in protein synthesis. *DSCR1<sup>-/-</sup>* growth cone, however, showed no local protein synthesis in the same condition. Furthermore, BDNF failed to induce protein synthesis in the presence of a translation inhibitor, anisomycin. Experiments were performed at DIV 3.  $n > 7$  axonal growth cones were analyzed for each condition. \*,  $P < 0.0003$ ; \*\*,  $P < 0.01$  compared with wild-type control. Values shown are mean  $\pm$  SEM and are tested for statistical significance by *t* test. Bar, 2  $\mu$ m.

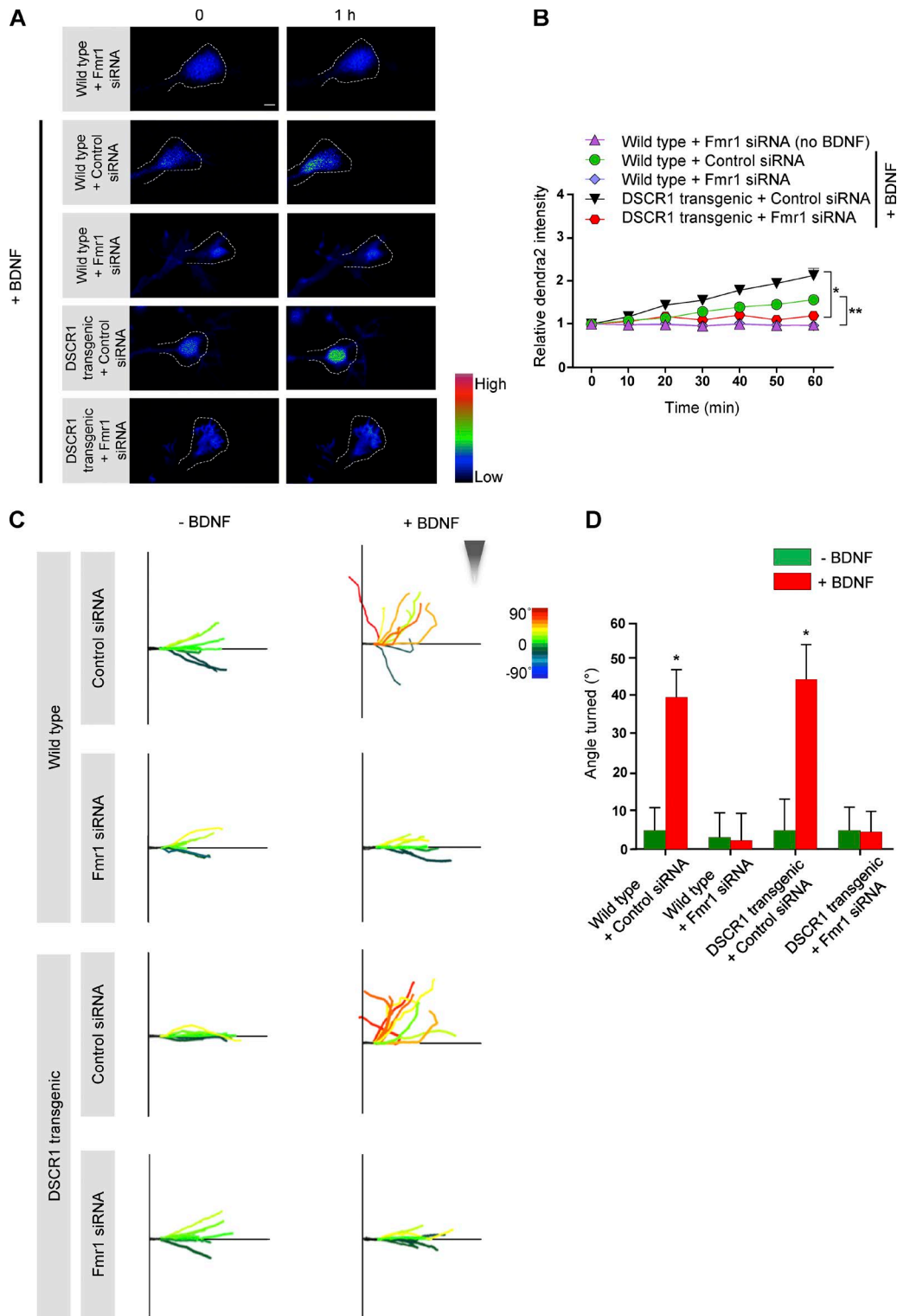


**Figure 6. FMRP reduction reduces local protein synthesis in growth cone and prevents axonal growth cone turning in wild-type and *DSCR1* transgenic neurons.** (A) Wild-type and *DSCR1* transgenic neurons were cotransfected with *dendra2*- $\beta$ -actin 3'UTR as well as control siRNA or *fmr1* siRNA. Increased intensity of *dendra2* represents BDNF-induced local protein synthesis in axonal growth cones. Bar, 2  $\mu$ m. (B) Axonal growth cones of wild-type and *DSCR1* transgenic neurons transfected with control siRNA showed high fluorescent intensity in response to BDNF treatment. In contrast, wild-type neurons transfected with *fmr1* siRNA showed no local protein synthesis. Furthermore, *DSCR1* transgenic neurons containing *fmr1* siRNA failed to translate *dendra2*- $\beta$ -actin 3'UTR reporter vector.  $n > 6$  axonal growth cones were analyzed for each condition. \*,  $P < 0.001$ ; \*\*,  $P < 0.004$ . (C) Trajectory plots show growth cone turning response of individual neurons of wild-type and *DSCR1* transgenic neurons transfected with control siRNA or *fmr1* siRNA.  $n = 10$  axonal growth cones were analyzed for each condition. (D) Axonal growth cones of wild-type or *DSCR1* transgenic neurons with reduced FMRP failed to turn toward BDNF. \*,  $P < 0.001$ . Values showed are mean  $\pm$  SEM and are tested for statistical significance by *t* test.

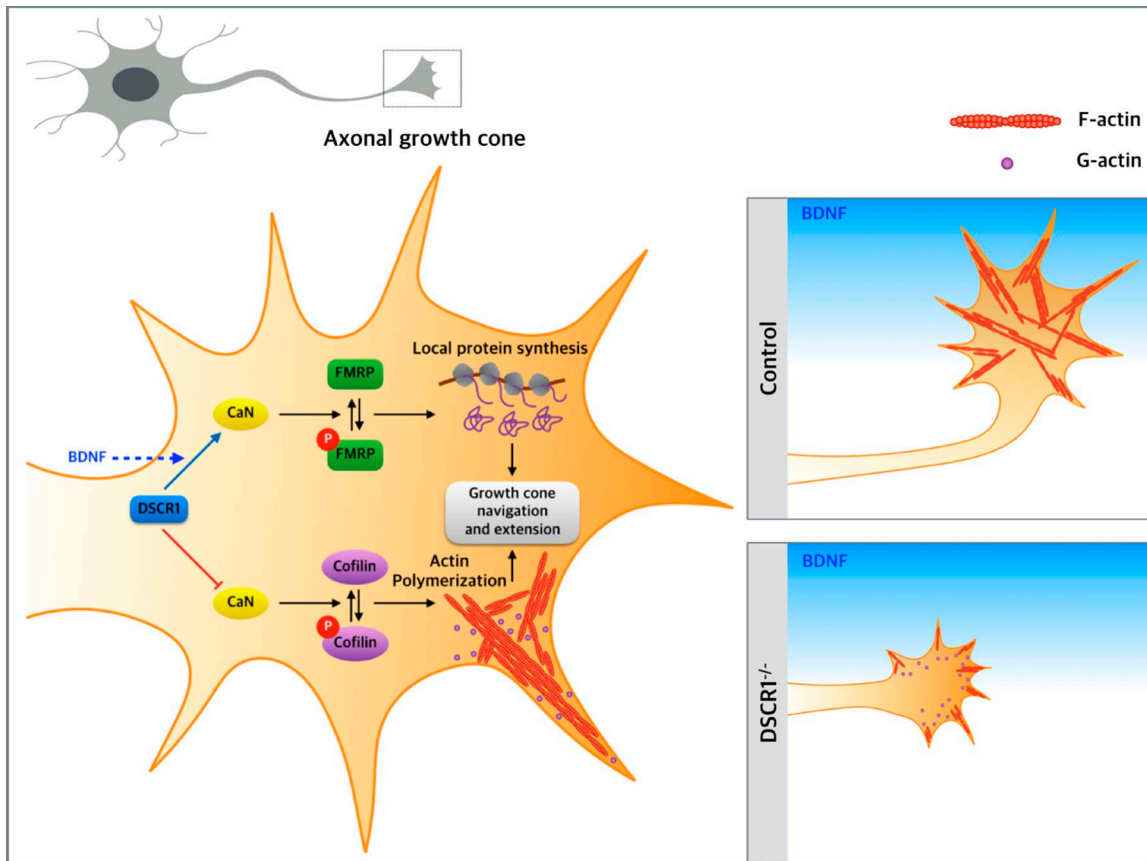


**Figure 7. A model shows the dual roles of DSCR1 in axonal growth cone.** DSCR1 mediates axonal growth cone extension and steering by regulating actin polymerization and local protein synthesis. During axonal growth cone advancement, DSCR1 regulates axon growth by modulating the activity of calcineurin that produces active cofilin to control actin polymerization. However, when axonal growth cone navigates to its target regions responding to signal cues, such as BDNF, DSCR1 becomes a key player in local protein synthesis by changing the status of FMRP phosphorylation, which mediates growth cone turning.

wild-type growth cones, and the increase in fluorescence was abrogated by anisomycin, an inhibitor of translation, suggesting that the BDNF-induced increase in fluorescence resulted from local protein synthesis. In the growth cones of *DSCR1*<sup>-/-</sup> neurons, BDNF treatment failed to induce new protein synthesis, whereas in *DSCR1* transgenic (*DSCR1*-overexpressing) growth cones, local protein synthesis was significantly enhanced compared with wild type. It is unlikely that the increase in green fluorescence is caused by diffusion of dendra-2 from the cell body because we confirmed that dendra-2 proteins in the cell body or axon projection do not reach axonal growth cones during the experimental time period (Fig. S4 B). Together, these results indicate that DSCR1 is required for BDNF-induced local  $\beta$ -actin mRNA translation in axonal growth cones.

#### DSCR1 regulates local $\beta$ -actin mRNA translation in axonal growth cones through FMRP

To further elucidate how DSCR1 regulates BDNF-induced local  $\beta$ -actin mRNA translation in axonal growth cones, we examined whether DSCR1 controls local protein synthesis through FMRP. Reasons for this are based on previous studies showing (a) FMRP localization at the axonal growth cone (Antar et al., 2006), (b) DSCR1 interacts with FMRP (Wang et al., 2012), and (c) FMRP associates with ZBP1, a protein that affects  $\beta$ -actin mRNA transport as well as translation (Rackham and Brown, 2004; Welshhans and Bassell, 2011). We found that

BDNF-dependent  $\beta$ -actin mRNA translation in axonal growth cone was significantly inhibited by *fmr1* siRNA transfection into wild-type and *DSCR1* transgenic hippocampal primary neurons (Fig. 6, A and B; and Fig. S4 C–E). Additionally, growth cone steering toward BDNF was also significantly inhibited (Fig. 6, C and D). Next, we examined whether DSCR1 controls the phosphorylation status of FMRP in axonal growth cones. Because calcineurin dephosphorylates phosphorylated FMRP upon BDNF treatment (Wang et al., 2012), we measured phosphorylated and dephosphorylated FMRP levels in growth cones of wild-type, *DSCR1*-deficient, and *DSCR1*-overexpressing neurons before and after BDNF treatment (Fig. S5). BDNF treatment reduced the levels of phosphorylated FMRP in the growth cones of wild-type and *DSCR1*-overexpressing neurons, but did not alter the level of phosphorylated FMRP in growth cones lacking *DSCR1*. This is consistent with our previous findings in dendritic spines because BDNF activates calcineurin via release from DSCR1-mediated inhibition. BDNF application to wild-type and *DSCR1*-overexpressing growth cones is expected to decrease phospho-FMRP by activating calcineurin, whereas the absence of DSCR1 in *DSCR1*<sup>-/-</sup> neurons is expected to be ineffective. Furthermore, we found that dephospho-FMRP is also reduced in axonal growth cones of wild-type and *DSCR1* transgenic neurons. This result is consistent with a previous study which showed that dephosphorylation induced rapid degradation of dephospho-FMRP by the ubiquitin-proteasome system (Nalavadi et al., 2012).

## Discussion

In summary, we have shown that DSCR1 plays a crucial role in developing axons by controlling both axon growth and guidance: (a) DSCR1 regulates local cytoskeletal dynamics in the growth cone, which is essential for axon outgrowth; and (b) DSCR1 controls local protein synthesis of  $\beta$ -actin in the growth cone, a process that is crucial for growth cone steering toward BDNF (Fig. 7). In contrast with ZBP1 that mediates local protein synthesis and growth cone turning, but does not alter axon growth (Welshans and Bassell, 2011), DSCR1 regulates both processes. Axonal growth cone turning is impeded in neurons lacking DSCR1, whereas neurons overexpressing *DSCR1* show excessive axonal growth cone turning mediated by increased local protein synthesis, particularly of  $\beta$ -actin. In addition, the axons of neurons lacking DSCR1 display delayed axon development, whereas those of neurons overexpressing *DSCR1* extended at a faster rate. Our work reveals that DSCR1 regulates axon outgrowth through its ability to regulate cofilin/phospho-cofilin ratio through calcineurin inhibition. In conclusion, our study reveals an important role of DSCR1 in local information processing in axonal growth cones: through regulation of local protein synthesis and cytoskeletal dynamics to control the rate and direction of axon growth. Because DSCR1 has been associated with various clinical manifestations in Down syndrome (Chang et al., 2003, 2013; Chang and Min, 2005; Hoeffer et al., 2007; Dierssen et al., 2011; Wang et al., 2012; Shaw and Chang, 2013), Fragile X syndrome (Wang et al., 2012; Chang et al., 2013), as well as in Alzheimer's disease (Shaw and Chang, 2013; Shaw et al., 2015), investigating the many roles of DSCR1 in neurons could shed new insights into the cellular and molecular mechanisms underlying developmental defects found in various neurologic disorders.

## Materials and methods

### Animals

Animals were used in accordance with protocols approved by the Animal Care and Use Committees of the Ulsan National Institute of Science and Technology. *DSCR1*<sup>-/-</sup> and *DSCR1* transgenic mice were obtained from K. Baek (Sungkyunkwan University, Seoul, South Korea). C57BL/6 mouse strain was purchased from Hyochang Science. All mutant mice used in this paper have the C57BL/6 strain background and have been confirmed by genotyping.

### Cell culture

Throughout this paper hippocampal primary neurons at DIV 2 or 3 were used as indicated. Hippocampal neuronal culture was prepared as previously described (Wang et al., 2012). In brief, hippocampi were dissected from E18 mouse embryos, followed by trypsin treatment. A 24-well plate containing 12-mm glass coverslips or 6-well plate containing 18-mm square glass coverslips (In Vitro Scientific) coated with poly-D-lysine (50  $\mu$ g/ml) were used for seeding neurons. Lipofectamine 2000 (Invitrogen) and Interferin (Polyplus Transfection) were used to transfect neurons with DNA and rhodamine 110 (Rho110)/Cy3-labeled tRNA, respectively.

### Plasmids constructions and preparation

Two repeats of *GAP-43* palmitoylation sequence and the mouse  $\beta$ -actin 3'UTR were inserted into the *pDendra2-C* vector (Evrogen) to create *pPalx2-Dendra2- $\beta$ -actin* 3'UTR. Lite-actin-EGFP vector was purchased from Ibidi. *pEGFP-cofilin* plasmid was purchased from

Addgene, and *Fmr1* siRNA and control siRNA were purchased from Santa Cruz Biotechnology, Inc.

### Immunocytochemistry

Hippocampal primary neurons were fixed in 4% paraformaldehyde and 0.25% glutaraldehyde in cytoskeleton buffer (10 mM MES, pH 6.1, 150 mM NaCl, 5 mM EGTA, 5 mM glucose, and 5 mM MgCl<sub>2</sub>) for 15 min at 37°C, and then treated twice with freshly prepared 0.1% (wt/vol) sodium borohydride for 10 min to reduce background fluorescence. Next, PBS washing was done for 10 min at RT, followed by 0.2% Triton X-100 in PBS for 10 min. Neurons were then blocked for 1 h at RT with PBS containing 1% BSA. Immunostaining was performed by applying primary antibodies as indicated (overnight at 4°C), followed by addition of Alexa Fluor-conjugated secondary antibodies (1:2,000; Invitrogen) for 1 h at RT. Images were taken with LSM780 (confocal; ZEISS) or Elyra S.1 (structured illumination microscopy; ZEISS). Primary antibodies used in this paper are as follows: DSCR1 polyclonal antibody (1:250; Abgent), MAP2 polyclonal antibody (1:10,000; Abcam), tau-1 monoclonal antibody (1:500; EMD Millipore),  $\beta$ -tubulin monoclonal antibody (1:500; Sigma-Aldrich), cofilin antibody (1:150; Abcam), and phospho-cofilin antibody (1:150; Abcam). We also used Alexa Fluor 488- or 555-conjugated Phalloidin dye to label actin filaments.

### Monomeric G-actin and actin filaments staining and analysis

Hippocampal primary neurons were fixed and washed as described in the Immunocytochemistry section. After permeabilization and blocking, neurons were incubated with DBP (10  $\mu$ g/ml; EMD Millipore) in PBS at RT for 1 h, followed by PBS washing and anti-DBP antibody (Dako) incubation. Images were acquired with Elyra S.1 (structured illumination microscopy) and then processed and analyzed using ZEN (ZEISS), ImageJ, and Metamorph (Molecular Devices) software. Ratio images were generated using Metamorph software as described previously (Lee et al., 2013). Profiles of the F-actin/G-actin ratio in filopodia was obtained and analyzed by drawing lines from the leading edge to the adjacency center zone of the growth cone and then averaged.

### Axon growth cone steering assay using Dunn chamber

Hippocampal neurons were plated on 18-mm square coverslips (Thermo Fisher Scientific), and the BDNF gradient was established by adding it to the outer well of the Dunn chamber. Images were taken every 5 min for 2 h. Dunn chamber axon guidance assays and analyses were performed as reported previously (Yam et al., 2009). During Dunn chamber assay, 5  $\mu$ M CsA was added as indicated.

### Long-term live imaging

Hippocampal neurons isolated from wild-type, *DSCR1*<sup>-/-</sup>, and *DSCR1* transgenic mice were transfected with EGFP or RFP-actin and *lifefact-GFP* to monitor the growth of axons. Live cell imaging was performed in an environmental chamber maintaining 37°C and 5% CO<sub>2</sub> throughout the experiment. Images were taken every hour for 12 h (for EGFP) or every 5 s for 10 min (for RFP-actin and *lifefact-GFP*) using a confocal microscope (LSM780; ZEISS) with a 40 $\times$  oil objective (NA 1.3, Plan Apo; Nikon) at 5-s intervals for 10 min.

### Superresolution microscope images

Structured illumination microscopy (Elyra S.1; ZEISS) was used to obtain super-resolution images. For structured illumination microscopy images, hippocampal neurons were fixed and treated with sodium borohydride and stained with antibodies as described in the Immunocytochemistry section. 1.21- $\mu$ m Z-stacks of high-resolution image frames were collected in three rotations with 488-, 561-, and 633-nm lasers. Images were then reconstructed using the ZEN software.

### tRNA FRET assay

Total yeast tRNAs, obtained from Anima Biotech, were labeled at dihydrouridine positions with either Rho110 or Cy3, as previously described (Barhoom et al., 2011), to yield fluorescent-labeled tRNAs. DIV 2 neurons were transfected with fluorescent-labeled tRNAs labeled with Rho110 or Cy3 using Interferin (Polyplus Transfection), and FRET assay was performed on DIV 3 neurons. FRET signals were measured after 1 h of BDNF treatment. Neurons transfected with tRNAs were treated with BDNF in the presence or absence of puromycin (0.5 mM; Cayman Chemical) for 1 h. Next, acceptor photobleaching experiment was performed for FRET efficiency analysis by using the LSM780 confocal microscope. The red fluorescence (561 nm) of the acceptor was bleached in axonal growth cones, and the intensity of donor green fluorescence (488 nm) was detected before and after photobleaching of the acceptor. FRET efficiency was determined by using the FRET acceptor bleaching analysis module in the ZEN imaging software, using the following equation:

$$\text{Efficiency (\%)} = \frac{D_{\text{Post}} - D_{\text{Pre}}}{D_{\text{Post}}} \times 100.$$

$D_{\text{Pre}}$  represents donor fluorescent intensity of the region before bleaching and  $D_{\text{Post}}$  shows the fluorescent intensity of the donor in the post-bleaching image. Note that only a subpopulation of active ribosomes will harbor a donor (acceptor FRET tRNA pair), as other configurations (e.g., wild type/donor, donor/donor, etc.) occur in parallel.

### Local mRNA translation assay

Cultured hippocampal neurons were transfected with *pPalx2-Dendra2-β-actin* 3'UTR reporter at DIV 2, and the translational assay was performed 24 h after the transfection, similar to previous work (Wang et al., 2012). In brief, neurons were exposed to human BDNF (30 ng/ml; Almond Labs) or translation inhibitor, anisomycin (10 μM; Almond Labs). The dendra-2 protein in growth cones was photoconverted, and images were taken every 10 min for 1 h.

### Statistical analysis

Statistical values shown are mean  $\pm$  SEM. Statistical significance was measured by *t* test using Prism 5.0 software (GraphPad Software).

### Online supplemental material

Fig. S1 shows that DSCR1 is present in the axonal growth cone. Fig. S2 shows the effect of CsA on the level of cofilin and phospho-cofilin in wild-type and *DSCR1* transgenic growth cone, as well as on F-actin/G-actin ratio of wild-type and *DSCR1* transgenic growth cone filopodia. Fig. S3 shows the effect of BDNF on the level of phospho-cofilin and cofilin in axonal growth cones of wild-type and *DSCR1*<sup>-/-</sup> neurons and the effect of wild-type *cofilin* and *cofilin S3E* overexpression on the ratio of cofilin/phospho-cofilin in wild-type neurons. Fig. S4 shows axonal growth cone turning in wild-type and *DSCR1* transgenic neurons transfected with *fmr1* siRNA. Fig. S5 shows the effect of BDNF on the level of phospho-FMRP and FMRP in axonal growth cones of wild-type, *DSCR1*<sup>-/-</sup>, and *DSCR1* transgenic neurons. Online supplemental material is available at <http://www.jcb.org/cgi/content/full/jcb.201510107/DC1>.

### Acknowledgments

We thank Ulsan National Institute of Science and Technology Olympus Biomed Imaging Center for super-resolution microscopy and K. Hong for preparing the summary model.

This work was supported by special research funds from Ulsan National Institute of Science and Technology (1.130054.01 and 1.150097.01) and a National Research Foundation of Korea grant funded by the Korean government (Ministry of Education, Science and Technology; 2012R1A2A2A01042981) to K.-T. Min; the Brain Research Program through the National Research Foundation of Korea funded by the Korean Ministry of Science, Information and Communications Technology, and Future Planning (NRF-2015M3C7A1028396) and Korea Institute of Science and Technology Young Fellow Program to E.-M. Hur; and grants from the National Institutes of Health (NS080946), Alzheimer's Association, and Global Down Syndrome Foundation to K.T. Chang.

The authors declare no competing financial interests.

Submitted: 27 October 2015

Accepted: 22 April 2016

### References

Aizawa, H., S. Wakatsuki, A. Ishii, K. Moriyama, Y. Sasaki, K. Ohashi, Y. Sekine-Aizawa, A. Sehara-Fujisawa, K. Mizuno, Y. Goshima, and I. Yahara. 2001. Phosphorylation of cofilin by LIM-kinase is necessary for semaphorin 3A-induced growth cone collapse. *Nat. Neurosci.* 4:367–373. <http://dx.doi.org/10.1038/86011>

Antar, L.N., C. Li, H. Zhang, R.C. Carroll, and G.J. Bassell. 2006. Local functions for FMRP in axon growth cone motility and activity-dependent regulation of filopodia and spine synapses. *Mol. Cell. Neurosci.* 32:37–48. <http://dx.doi.org/10.1016/j.mcn.2006.02.001>

Arron, J.R., M.M. Winslow, A. Polleri, C.-P. Chang, H. Wu, X. Gao, J.R. Neilson, L. Chen, J.J. Heit, S.K. Kim, et al. 2006. NFAT dysregulation by increased dosage of DSCR1 and DYRK1A on chromosome 21. *Nature*. 441:595–600. <http://dx.doi.org/10.1038/nature04678>

Barhoom, S., J. Kaur, B.S. Cooperman, N.I. Smorodinsky, Z. Smilansky, M. Ehrlich, and O. Elroy-Stein. 2011. Quantitative single cell monitoring of protein synthesis at subcellular resolution using fluorescently labeled tRNA. *Nucleic Acids Res.* 39:e129. <http://dx.doi.org/10.1093/nar/gkr01>

Brittis, P.A., Q. Lu, and J.G. Flanagan. 2002. Axonal protein synthesis provides a mechanism for localized regulation at an intermediate target. *Cell*. 110:223–235. [http://dx.doi.org/10.1016/S0092-8674\(02\)00813-9](http://dx.doi.org/10.1016/S0092-8674(02)00813-9)

Buck, K.B., and J.Q. Zheng. 2002. Growth cone turning induced by direct local modification of microtubule dynamics. *J. Neurosci.* 22:9358–9367.

Casas, C., S. Martínez, M.A. Pritchard, J.J. Fuentes, M. Nadal, J. Guimerà, M. Arbonés, J. Flórez, E. Sorianó, X. Estivill, and S. Alcántara. 2001. Dscr1, a novel endogenous inhibitor of calcineurin signaling, is expressed in the primitive ventricle of the heart and during neurogenesis. *Mech. Dev.* 101:289–292. [http://dx.doi.org/10.1016/S0925-4773\(00\)00583-9](http://dx.doi.org/10.1016/S0925-4773(00)00583-9)

Chang, K.T., and K.-T. Min. 2005. *Drosophila melanogaster* homolog of Down syndrome critical region 1 is critical for mitochondrial function. *Nat. Neurosci.* 8:1577–1585. <http://dx.doi.org/10.1038/nn1564>

Chang, K.T., Y.-J. Shi, and K.-T. Min. 2003. The *Drosophila* homolog of Down's syndrome critical region 1 gene regulates learning: implications for mental retardation. *Proc. Natl. Acad. Sci. USA*. 100:15794–15799. <http://dx.doi.org/10.1073/pnas.2536696100>

Chang, K.T., H. Ro, W. Wang, and K.T. Min. 2013. Meeting at the crossroads: common mechanisms in Fragile X and Down syndrome. *Trends Neurosci.* 36:685–694. <http://dx.doi.org/10.1016/j.tins.2013.08.007>

Dent, E.W., J.L. Callaway, G. Szebenyi, P.W. Baas, and K. Kalil. 1999. Reorganization and movement of microtubules in axonal growth cones and developing interstitial branches. *J. Neurosci.* 19:8894–8908.

Dent, E.W., S.L. Gupton, and F.B. Gertler. 2011. The growth cone cytoskeleton in axon outgrowth and guidance. *Cold Spring Harb. Perspect. Biol.* 3:3. <http://dx.doi.org/10.1101/cshperspect.a001800>

Dierssens, M., G. Arqué, J. McDonald, N. Andreu, C. Martínez-Cué, J. Flórez, and C. Fillat. 2011. Behavioral characterization of a mouse model overexpressing DSCR1/RCAN1. *PLoS One*. 6:e17010. <http://dx.doi.org/10.1371/journal.pone.0017010>

Endo, M., K. Ohashi, and K. Mizuno. 2007. LIM kinase and slingshot are critical for neurite extension. *J. Biol. Chem.* 282:13692–13702. <http://dx.doi.org/10.1074/jbc.M610873200>

Fishkind, D.J., and Y.L. Wang. 1993. Orientation and three-dimensional organization of actin filaments in dividing cultured cells. *J. Cell Biol.* 123:837–848. <http://dx.doi.org/10.1083/jcb.123.4.837>

Fuentes, J.J., M.A. Pritchard, A.M. Planas, A. Bosch, I. Ferrer, and X. Estivill. 1995. A new human gene from the Down syndrome critical region encodes a proline-rich protein highly expressed in fetal brain and heart. *Hum. Mol. Genet.* 4:1935–1944. <http://dx.doi.org/10.1093/hmg/4.10.1935>

Fuentes, J.J., L. Genescà, T.J. Kingsbury, K.W. Cunningham, M. Pérez-Riba, X. Estivill, and S. de la Luna. 2000. DSCR1, overexpressed in Down syndrome, is an inhibitor of calcineurin-mediated signaling pathways. *Hum. Mol. Genet.* 9:1681–1690. <http://dx.doi.org/10.1093/hmg/9.11.1681>

Görlach, J., D.S. Fox, N.S. Cutler, G.M. Cox, J.R. Perfect, and J. Heitman. 2000. Identification and characterization of a highly conserved calcineurin binding protein, CBP1/calcipressin, in *Cryptococcus neoformans*. *EMBO J.* 19:3618–3629. <http://dx.doi.org/10.1093/emboj/19.14.3618>

Hoeffner, C.A., A. Dey, N. Sachan, H. Wong, R.J. Patterson, J.M. Shelton, J.A. Richardson, E. Klann, and B.A. Rothermel. 2007. The Down syndrome critical region protein RCAN1 regulates long-term potentiation and memory via inhibition of phosphatase signaling. *J. Neurosci.* 27:13161–13172. <http://dx.doi.org/10.1523/JNEUROSCI.3974-07.2007>

Hsieh, S.H.K., G.B. Ferraro, and A.E. Fournier. 2006. Myelin-associated inhibitors regulate cofilin phosphorylation and neuronal inhibition through LIM kinase and Slingshot phosphatase. *J. Neurosci.* 26:1006–1015. <http://dx.doi.org/10.1523/JNEUROSCI.2806-05.2006>

Jung, H., B.C. Yoon, and C.E. Holt. 2012. Axonal mRNA localization and local protein synthesis in nervous system assembly, maintenance and repair. *Nat. Rev. Neurosci.* 13:308–324. <http://dx.doi.org/10.1038/nrn3274>

Kingsbury, T.J., and K.W. Cunningham. 2000. A conserved family of calcineurin regulators. *Genes Dev.* 14:1595–1604.

Kornack, D.R., and R.J. Giger. 2005. Probing microtubule +TIPs: regulation of axon branching. *Curr. Opin. Neurobiol.* 15:58–66. <http://dx.doi.org/10.1016/j.conb.2005.01.009>

Lee, C.W., E.A. Vitriol, S. Shim, A.L. Wise, R.P. Velayutham, and J.Q. Zheng. 2013. Dynamic localization of G-actin during membrane protrusion in neuronal motility. *Curr. Biol.* 23:1046–1056. <http://dx.doi.org/10.1016/j.cub.2013.04.057>

Leung, K.M., F.P. van Horck, A.C. Lin, R. Allison, N. Standart, and C.E. Holt. 2006. Asymmetrical beta-actin mRNA translation in growth cones mediates attractive turning to netrin-1. *Nat. Neurosci.* 9:1247–1256. <http://dx.doi.org/10.1038/nn1775>

Lowery, L.A., and D. Van Vactor. 2009. The trip of the tip: understanding the growth cone machinery. *Nat. Rev. Mol. Cell Biol.* 10:332–343. <http://dx.doi.org/10.1038/nrm2679>

Nalavadi, V.C., R.S. Muddashetty, C. Gross, and G.J. Bassell. 2012. Dephosphorylation-induced ubiquitination and degradation of FMRP in dendrites: a role in immediate early mGluR-stimulated translation. *J. Neurosci.* 32:2582–2587. <http://dx.doi.org/10.1523/JNEUROSCI.5057-11.2012>

Piper, M., R. Anderson, A. Dwivedy, C. Weinl, F. van Horck, K.M. Leung, E. Cogill, and C. Holt. 2006. Signaling mechanisms underlying Slit2-induced collapse of *Xenopus* retinal growth cones. *Neuron.* 49:215–228. <http://dx.doi.org/10.1016/j.neuron.2005.12.008>

Rackham, O., and C.M. Brown. 2004. Visualization of RNA-protein interactions in living cells: FMRP and IMP1 interact on mRNAs. *EMBO J.* 23:3346–3355. <http://dx.doi.org/10.1016/j.emboj.7600341>

Santoro, M.R., S.M. Bray, and S.T. Warren. 2012. Molecular mechanisms of fragile X syndrome: a twenty-year perspective. *Annu. Rev. Pathol.* 7:219–245. <http://dx.doi.org/10.1146/annurev-pathol-011811-132457>

Schaefer, A.W., N. Kabir, and P. Forscher. 2002. Filopodia and actin arcs guide the assembly and transport of two populations of microtubules with unique dynamic parameters in neuronal growth cones. *J. Cell Biol.* 158:139–152. <http://dx.doi.org/10.1083/jcb.200203038>

Schaefer, A.W., V.T. Schoonderwoert, L. Ji, N. Mederos, G. Danuser, and P. Forscher. 2008. Coordination of actin filament and microtubule dynamics during neurite outgrowth. *Dev. Cell.* 15:146–162. <http://dx.doi.org/10.1016/j.devcel.2008.05.003>

Shaw, J.L., and K.T. Chang. 2013. Nebula/DSCR1 upregulation delays neurodegeneration and protects against APP-induced axonal transport defects by restoring calcineurin and GSK-3 $\beta$  signaling. *PLoS Genet.* 9:e1003792. <http://dx.doi.org/10.1371/journal.pgen.1003792>

Shaw, J.L., S. Zhang, and K.T. Chang. 2015. Bidirectional regulation of amyloid precursor protein-induced memory defects by Nebula/DSCR1: A protein upregulated in Alzheimer's disease and Down syndrome. *J. Neurosci.* 35:11374–11383. <http://dx.doi.org/10.1523/JNEUROSCI.1163-15.2015>

Tcherkezian, J., P.A. Brittis, F. Thomas, P.P. Roux, and J.G. Flanagan. 2010. Transmembrane receptor DCC associates with protein synthesis machinery and regulates translation. *Cell.* 141:632–644. <http://dx.doi.org/10.1016/j.cell.2010.04.008>

Van Baelen, H., R. Bouillon, and P. De Moor. 1980. Vitamin D-binding protein (G<sub>c</sub>-globulin) binds actin. *J. Biol. Chem.* 255:2270–2272.

Vitriol, E.A., and J.Q. Zheng. 2012. Growth cone travel in space and time: the cellular ensemble of cytoskeleton, adhesion, and membrane. *Neuron.* 73:1068–1081. <http://dx.doi.org/10.1016/j.neuron.2012.03.005>

Wang, W., J.Z. Zhu, K.T. Chang, and K.T. Min. 2012. DSCR1 interacts with FMRP and is required for spine morphogenesis and local protein synthesis. *EMBO J.* 31:3655–3666. <http://dx.doi.org/10.1038/embj.2012.190>

Wang, Y., F. Shibusaki, and K. Mizuno. 2005. Calcium signal-induced cofilin dephosphorylation is mediated by Slingshot via calcineurin. *J. Biol. Chem.* 280:12683–12689. <http://dx.doi.org/10.1074/jbc.M411494200>

Welshhans, K., and G.J. Bassell. 2011. Netrin-1-induced local  $\beta$ -actin synthesis and growth cone guidance requires zipcode binding protein 1. *J. Neurosci.* 31:9800–9813. <http://dx.doi.org/10.1523/JNEUROSCI.0166-11.2011>

Willis, D.E., E.A. van Niekerk, Y. Sasaki, M. Mesngon, T.T. Merienda, G.G. Williams, M. Kendall, D.S. Smith, G.J. Bassell, and J.L. Twiss. 2007. Extracellular stimuli specifically regulate localized levels of individual neuronal mRNAs. *J. Cell Biol.* 178:965–980. <http://dx.doi.org/10.1083/jcb.200703209>

Yam, P.T., S.D. Langlois, S. Morin, and F. Charron. 2009. Sonic hedgehog guides axons through a noncanonical, Src-family-kinase-dependent signaling pathway. *Neuron.* 62:349–362. <http://dx.doi.org/10.1016/j.neuron.2009.03.022>

Yao, J., Y. Sasaki, Z. Wen, G.J. Bassell, and J.Q. Zheng. 2006. An essential role for beta-actin mRNA localization and translation in Ca<sup>2+</sup>-dependent growth cone guidance. *Nat. Neurosci.* 9:1265–1273. <http://dx.doi.org/10.1038/nn1773>

Zhou, Q., K.J. Homma, and M.M. Poo. 2004. Shrinkage of dendritic spines associated with long-term depression of hippocampal synapses. *Neuron.* 44:749–757. <http://dx.doi.org/10.1016/j.neuron.2004.11.011>